IEEE Access
Multidisciplinary | Rapid Review | Open Access Journal

Received November 22, 2018, accepted December 8, 2018, date of publication December 12, 2018,
date of current version January 4, 2019.

*Digital Object Identifier 10.1109/ACCESS.2018.2886397*

# Efficient and Accurate Detection and Frequency Estimation of Multiple Sinusoids

**SLOBODAN DJUKANOVIĆ, (Member, IEEE), AND VESNA POPOVIĆ-BUGARIN, (Member, IEEE)**
Faculty of Electrical Engineering, Džordža Vašingtona bb, University of Montenegro, 81000 Podgorica, Montenegro

Corresponding author: Slobodan Djukanović (slobdj@ucg.ac.me)

**ABSTRACT** The method for detection of complex sinusoids in additive white Gaussian noise and estimation of their frequencies is proposed. It contains two stages: 1) sinusoid detection (model order estimation) and coarse frequency estimation, and 2) fine frequency estimation. The proposed method operates in the frequency domain, i.e., it uses the discrete Fourier transform (DFT) as the main tool. Sinusoid detection is performed so that a fixed probability of false alarm is provided (Neymann–Pearson criterion). For both coarse and fine frequency estimations, the three-point periodogram maximization approach is used. Simulations are carried out for variable signal-to-noise ratio, variable frequency displacement between the sinusoids and variable offset from the frequency grid. The proposed method meets the Cramér–Rao lower bound in frequency estimation and practically does not depend on the frequency displacement except for very small displacement values. In terms of model order estimation accuracy, it outperforms the state-of-the-art approaches. The most expensive operation in the method is the calculation of the DFT. Therefore, in terms of calculation complexity, the proposed method is on par with the most efficient algorithms for multiple frequency estimations.

**INDEX TERMS** Cramér-Rao lower bound, discrete Fourier transform, model order estimation, multiple frequency estimation, Neymann-Pearson criterion.

## I. INTRODUCTION

Frequency estimation of multiple sinusoids, also known as line spectral estimation, represents a fundamental problem that arises in numerous applications, including power systems [1], signal processing [2], [3], telecommunications [4]–[7], global position systems [8], biomedical engineering [9], mechanical engineering [10]. In telecommunications, for example, frequency estimation of multiple sinusoids is encountered in channel estimation of mm-wave MIMO systems [4], [5], carrier frequency offset estimation in OFDM systems [6], frequency estimation for burst mode communications [7] etc. Maximum likelihood (ML) estimator of the frequencies of multiple sinusoids is asymptotically efficient for additive white Gaussian noise (AWGN) and exhibits good performance for non-Gaussian noise [2]. However, its numerical implementation through standard techniques is very complex [11] and therefore other suboptimal estimators, based on the discrete Fourier transform (DFT) [12] or subspace techniques such as multiple signal classification (MUSIC) [13] and estimation of signal parameters via rotational invariance techniques (ESPRIT) [14], are commonly used. The main advantage of the MUSIC and ESPRIT methods over DFT is superresolution, i.e. the ability to estimate the frequencies with resolution higher than one DFT bin. On the other side, their disadvantage is that they require the number of sinusoids to be known in advance, restricting their use in more general cases. One recent contribution that uses the MUSIC-based approach on the undersampled data is proposed in [15]. A numerical implementation of the ML estimator has been proposed in [16]. Initial frequency estimations in [16] are computed using the DFT and refined via the modified variable projection.

The DFT-based approach is particularly popular since, in the case of single complex sinusoid embedded in AWGN, the ML frequency estimation is obtained by maximizing its periodogram [17], which can be efficiently computed using the DFT. Therefore, the most popular single frequency estimators are based on the periodogram maximization through some form of interpolation in the frequency domain [18]–[24]. When dealing with multiple sinusoids, the DFT is not an optimal solution due to the spectral leakage effect, which can be alleviated by applying windowing in the time domain [1], [12]. However, a non-negligible frequency bias still remains after windowing [22]. The case of single real-valued sinusoid is equivalent to the case of two complex sinusoids with the same amplitudes and opposite



2169-3536 © 2018 IEEE. Translations and content mining are permitted for academic research only.
Personal use is also permitted, but republication/redistribution requires IEEE permission.
See http://www.ieee.org/publications_standards/publications/rights/index.html for more information.

sign frequencies [22]. However, due to the spectrum symmetry of real-valued signals, the periodogram-based frequency estimation of a real-valued sinusoid is performed by maximizing only one spectral peak (at positive or negative frequencies) [11].

This paper presents a joint solution for detection of complex sinusoids (cisoids) embedded in AWGN and estimation of their frequencies. Detection (model order estimation) and frequency estimation are performed in the frequency domain. The strongest peaks are detected and removed from the spectrum, one at a time, until we conclude that the remaining spectrum does not contain peaks that can be associated with cisoids. That conclusion is made so that a fixed probability of false alarm (PFA) is provided, i.e. according to the Neymann-Pearson criterion. Along with model order estimation, coarse frequency estimations are obtained, which are improved in the estimation refinement stage. Simulations show that the frequency estimation accuracy meets the Cramér-Rao lower bound (CRLB). Both model order and frequency estimation are based on the standard DFT, which enables efficient implementation of the proposed method. In terms of calculation complexity, it is on par with the most efficient state-of-the-art algorithms [24]. As opposed to [24]: i) we do not assume that the model order is known a priori and ii) our approach does not suffer from the error saturation effect at higher signal-to-noise ratio (SNR). In terms of model order estimation, it outperforms the state-of-the-art approaches [25], [26] in both accuracy and efficiency.

In Section II, the signal model and the problem statement are given. The proposed method for detection and frequency estimation of multiple cisoids is described in Section III, whereas its performance is evaluated in Section IV. Conclusions are drawn in Section V.

## II. PROBLEM DESCRIPTION

Let us consider the following received signal:

$$x(n) = \sum_{k=1}^{K} A_k e^{j(2\pi f_k n + \phi_k)} + \epsilon(n), \quad n = 0, 1, \cdots, N-1, \tag{1}$$

where $A_k$, $f_k$ and $\phi_k$ represent the amplitude, frequency and initial phase of the $k$-th complex sinusoid, respectively, $K$ the unknown number of complex sinusoids (model order), $\epsilon(n)$ zero-mean AWGN with variance $\sigma_\epsilon^2$ and $N$ the signal length. In addition, $A_k > 0$ and $|f_k| < 1/2$ for $k = 1, 2, \ldots, K$, whereas $\phi_k$ are independent random variables uniformly distributed within $(-\pi, \pi]$. Since the periodogram-based methods cannot resolve peaks separated by less than $1/N$ in cycles per sampling interval [11, Sec. 2.4.1], we will assume that sinusoids are at least one DFT bin apart. Our aim is to estimate the model order $K$ and sinusoid frequencies $f_k$.

Relation (1) can be written in matrix form as [11], [16]

$$\mathbf{x} = \Phi\mathbf{a} + \epsilon, \tag{2}$$

where

$$\Phi = \begin{bmatrix} 1 & 1 & \cdots & 1 \\ e^{j2\pi f_1} & e^{j2\pi f_2} & \cdots & e^{j2\pi f_k} \\ \vdots & \vdots & \ddots & \vdots \\ e^{j2\pi(N-1)f_1} & e^{j2\pi(N-1)f_2} & \cdots & e^{j2\pi(N-1)f_k} \end{bmatrix}_{N\times K} \tag{3}$$

$$\mathbf{a} = \begin{bmatrix} A_1 e^{j\phi_1} & A_2 e^{j\phi_2} & \cdots & A_K e^{j\phi_K} \end{bmatrix}^T \tag{4}$$

$$\epsilon = \begin{bmatrix} \epsilon(0) & \epsilon(1) & \cdots & \epsilon(N-1) \end{bmatrix}^T. \tag{5}$$

The ML estimate of the frequency vector $\mathbf{f} = [f_1 f_2 \cdots f_K]^T$ is given by [11], [16]

$$\hat{\mathbf{f}} = \arg\max_{\mathbf{f}} L(\mathbf{f}), \tag{6}$$

with

$$L(\mathbf{f}) = \mathbf{x}^H \Phi(\Phi^H\Phi)^{-1}\Phi^H\mathbf{x}, \tag{7}$$

where $()^H$ represents the Hermitian transpose operator.

Unfortunately, maximization of $L(\mathbf{f})$ is difficult to achieve due to its complicated multimodal shape with sharp global maxima corresponding to vector $\mathbf{f}$ [2]. Finding $\hat{\mathbf{f}}$ requires a stable and accurate initialization, which is currently not available in the literature [11]. Therefore, the initialization is usually performed using the DFT approach, which is further refined by other iterative techniques [16].

The CRLBs for frequencies, amplitudes and initial phases of multiple cisoids are derived in [12]. The exact analytical CRLB expression for $f_k$ in general case is not available. However, it can be shown that the asymptotic CRLB (as $N \to \infty$) for frequency estimation $\hat{f}_k$ satisfies [11]

$$\mathrm{var}(\hat{f}_k) \geq \frac{6\sigma_\epsilon^2}{N^3 A_k^2}. \tag{8}$$

## III. PROPOSED METHOD

In this section, we present a joint solution for the estimation of the number of complex sinusoids embedded in AWGN and their frequencies. The proposed method contains two stages: i) detection and coarse frequency estimation and ii) fine frequency estimation. The stages are described in the sequel.

### A. DETECTION AND COARSE FREQUENCY ESTIMATION

Detection of sinusoids (spectral lines) starts with the strongest one. After locating that component and obtaining its coarse frequency estimation, say $f_k^c$ ($c$ stands for *coarse*), we remove it from $x(n)$ via the following three steps:

1) Demodulate $x(n)$ by $e^{-j2\pi f_k^c n}$: $x^d(n) = x(n)e^{-j2\pi f_k^c n}$ ($d$ in $x^d(n)$ stands for *demodulation*).
2) Remove the DC component of $x^d(n)$.
3) Modulate $x^d(n)$ to obtain the signal $x(n)$ without the strongest component: $x^\dagger(n) = x^d(n)e^{j2\pi f_k^c n}$.

If $f_k^c$ is accurate enough, the strongest component will be located at low-frequency band of $x^d(n)$ after the first step. Ideally, it will occupy only the DC component of $x^d(n)$. After the second step, the greatest portion of its energy will be removed. Finally, the third step cancels the demodulation effect of the first step. The estimation accuracy of $f_k^c$ will be discussed shortly.

Steps 1–3 are repeated until we conclude that the spectrum of $x^\dagger(n)$ does not contain any spectral lines that can be associated with cisoids. After each component removal, maximum of the remaining spectrum is compared to a predefined threshold $T$. If it exceeds the value of $T$, we conclude that additional cisoids exist in the spectrum and repeat the procedure. The value of $T$ is determined so that a fixed PFA is provided (Neymann-Pearson criterion). To that end, assume that the spectrum does not contain sinusoids, i.e. that it contains only the noise. Since $\epsilon(n)$ is AWGN with i.i.d. real and imaginary parts, the DFT of $\epsilon(n)$, denoted as $E(m)$, where $m = 0, 1, \cdots, N-1$ is discrete frequency index, is also complex AWGN with zero mean and variance $N\sigma_\epsilon^2$ [11]. Modulus of $E(m)$ is a Rayleigh variable with scale parameter

$$b_{|E|} = \sqrt{\frac{N}{2}}\sigma_\epsilon. \tag{9}$$

The mean and variance of $|E(m)|$ are defined as [27]

$$\begin{aligned}\mu_{|E|} &= \sqrt{\frac{\pi}{2}}b_{|E|}\\ \sigma_{|E|}^2 &= \left(2-\frac{\pi}{2}\right)b_{|E|}^2.\end{aligned} \tag{10}$$

For example, the PFAs corresponding to $T = \mu_{|E|} + 3\sigma_{|E|}$, $\mu_{|E|} + 4\sigma_{|E|}$ and $\mu_{|E|} + 5\sigma_{|E|}$, are $P(|E| \geq T) = 5.628 \times 10^{-3}$, $5.512 \times 10^{-4}$ and $3.515 \times 10^{-5}$, respectively.

Parameter $b_{|E|}$, and hence $\mu_{|E|}$ and $\sigma_{|E|}$, can be estimated from the DFT of $x(n)$. Since the DFT of a white-noise process is also a white-noise process and since the white noise is distributed uniformly in frequency, as opposed to sinusoids which occupy very narrow frequency bands, $b_{|E|}$ can be estimated from the DFT bins not occupied by sinusoids. Alternatively, we can use a time-frequency approach [28].

The sinusoid detection performance depends on the estimation accuracy of $f_k^c$. If the estimation is not accurate enough, the current strongest component will not be properly removed, i.e. a significant part of its energy will remain [28], which can degrade the performance of detection of other sinusoids. Therefore, it is essential to use accurate frequency estimator for this purpose. In this method, we will use a low-complexity single-cisoid frequency estimator proposed in [29], which achieves the CRLB. Section III-C gives a brief description of this estimator. The frequency estimations obtained in this stage represent coarse estimations and will be refined using the procedure described in Section III-B.

Finally, the three step procedure for removing the current strongest cisoid from the received signal can be performed very efficiently, without calculating the DFT [22]. Since the DC component of $x^d(n)$ equals the sum of its samples, the signal $x^\dagger(n)$ can be obtained simply as

$$\begin{aligned}x^\dagger(n) &= \left[x^d(n) - \overline{x^d(n)}\right]e^{j2\pi f_k^c n}\\ &= x(n) - \overline{x^d(n)}e^{j2\pi f_k^c n},\end{aligned} \tag{11}$$

where $\overline{x^d(n)}$ represents the mean value of $x^d(n)$. In (11), term $x^d(n) - \overline{x^d(n)}$ within brackets corresponds to Step 2 in the procedure given at the beginning of this section.

### B. FINE FREQUENCY ESTIMATION

Once the model order estimation $\hat{K}$ and coarse frequencies $f_k^c$, $k = 1, 2, \cdots, \hat{K}$, are obtained, the fine frequency estimation is performed as follows:

1) Set $f_k^r = f_k^c$ for every $k = 1, 2, \cdots, \hat{K}$ ($r$ stands for *refined*).
2) For every $k$, $k = 1, 2, \cdots, \hat{K}$, do
   a) Remove all the sinusoids from the considered signal, except the $k$-th one, following the procedure described in section III-A with estimations $f_k^r$, $k = 1, 2, \cdots, \hat{K}$.
   b) Refine the frequency estimation of the $k$-th sinusoid and update $f_k^r$ with the obtained value.

In order to mitigate the influence of other sinusoids on the one currently estimated [12], [22], we remove them from the considered signal. Then we use the periodogram maximization as the ML approach for single frequency estimation. Simulations show that sinusoid removal is crucial in improving the estimation accuracy to the CRLB limit.

### C. THREE-POINT PERIODOGRAM MAXIMIZATION

In this section, we briefly overview the frequency estimation method [29] used herein, incorporated in both coarse and fine frequency estimations.

The ML frequency estimation of a single cisoid is obtained as [17]

$$\hat{f}_{\mathrm{ML}} = \arg\max_\theta P(\theta), \tag{12}$$

where the periodogram $P(\theta)$ is defined as

$$P(\theta) = \left|\sum_{n=0}^{N-1} x(n)e^{-j2\pi\theta n}\right|. \tag{13}$$

$\theta$ represents continuous frequency. The periodogram is calculated via DFT, so the true periodogram maximum and the DFT maximum generally do not coincide. Method [29] comprises three steps for estimating the displacement $\delta$ between these two maxima, given as follows:

1) *Coarse estimation* Calculate the DFT of $x(n)$, denoted as $X(m)$, and locate the maximum position $m_0$.
2) *Candan's estimation* Calculate the Candan's displacement [20]

$$\hat{\delta}_C = \frac{\arctan\left(\tan(\frac{\pi}{N})\mathrm{Re}\left\{\frac{X(m_0-1)-X(m_0+1)}{2X(m_0)-X(m_0-1)-X(m_0+1)}\right\}\right)}{\frac{\pi}{N}}. \tag{14}$$

3) *Parabolic interpolation* Calculate three periodogram samples $P_1$, $P_2$ and $P_3$ at $\theta_1 = f_C - f_d$, $\theta_2 = f_C$ and

**Algorithm 1** Model Order and Frequency Estimation of Multiple Sinusoids

**Input** Algorithm input is the sequence $x(n)$, defined by (1), and the estimated noise variance. The threshold $T$ is calculated using the noise variance.

**Detection and coarse frequency estimation**

Calculate $X(m) = \text{DFT}[x(n)]$. Set $k = 0$, $x^{\dagger}(n) = x(n)$ and $X^{\dagger}(m) = X(m)$. Locate the maximum of $|X^{\dagger}(m)|$ as $m_0 = \arg\max_k |X^{\dagger}(m)|$.

`While` $|X^{\dagger}(m_0)| > T$ `do`

1) $k = k + 1$
2) Estimate the frequency of the $k$-th sinusoid from $x^{\dagger}(n)$, using the three-point periodogram maximization, to obtain the coarse estimation $f_k^c$.
3) Remove the $k$-th sinusoid component from $x^{\dagger}(n)$ by $x^{\dagger}(n) = x^{\dagger}(n) - \overline{x^d(n)} e^{j2\pi f_k^c n}$, where $x^d(n) = x^{\dagger}(n) e^{-j2\pi f_k^c n}$.
4) Calculate the DFT of $x^{\dagger}(n)$ and locate its maximum as $m_0 = \arg\max_k |X^{\dagger}(m)|$.

`Loop`

$\hat{K} = k$ represents the estimation of model order.

$f_k^c, k \in \{1, 2, \cdots, \hat{K}\}$, are coarse frequency estimations.

**Fine frequency estimation**

Set $f_k^r = f_k^c, k \in \{1, 2, \cdots, \hat{K}\}$.

`For every` $k \in \{1, 2, \cdots, \hat{K}\}$ `do`

1) Set $x^{\dagger}(n) = x(n)$.
2) `For every` $k_1 \in \{1, 2, \cdots, \hat{K}\} \setminus \{k\}$ `do` Remove the $k_1$-th sinusoid from $x^{\dagger}(n)$ as $x^{\dagger}(n) = x^{\dagger}(n) - \overline{x^d(n)} e^{j2\pi f_{k_1}^r n}$, where $x^d(n) = x^{\dagger}(n) e^{-j2\pi f_{k_1}^r n}$. `Next` $k_1$
3) Refine the frequency estimation of the $k$-th component using the three-point periodogram maximization and update $f_k^r$ with the obtained value.

`Next` $k$

**Output** Algorithm outputs are $\hat{K}$ and $f_k^r$, $k \in \{1, 2, \cdots, \hat{K}\}$.

$\theta_3 = f_C + f_d$, respectively. The central frequency is calculated as $f_C = (m_0 + \hat{\delta}_C)/N$, where $\hat{\delta}_C$ is given by (14). Side frequencies $\theta_1$ and $\theta_3$ are displaced by $f_d$ from $f_C$, and $f_d$ can be chosen arbitrarily in interval $(0, \frac{1}{2N}]$, without affecting the method's performance [29]. The final frequency estimation is obtained as the vertex of a parabola fitted through points $(\theta_1, P_1)$, $(\theta_2, P_2)$ and $(\theta_3, P_3)$ [29], i.e.

$$\theta_{fin} = \frac{1}{2} \frac{\theta_3^2(P_1 - P_2) + \theta_2^2(P_3 - P_1) + \theta_1^2(P_2 - P_3)}{\theta_3(P_1 - P_2) + \theta_2(P_3 - P_1) + \theta_1(P_2 - P_3)}. \tag{15}$$

### D. OVERALL ALGORITHM

Algorithms presented in Sections III-A and III-B are combined into an integral algorithm, Algorithm 1, which also includes the DC removal approach (11) and other implementation details. The algorithm is given at the beginning of this page.

### E. CALCULATION COMPLEXITY

In complexity analysis, we neglect all operations with $O(1)$ complexity, where $O(\cdot)$ represents big O notation, i.e. we neglect all complexity terms not depending on $N$. From the proposed algorithm, we may conclude that the sinusoid detection and coarse frequency estimation step requires the calculation of $\hat{K} + 1$ DFTs, $\hat{K} + 1$ DFT maximum detections, calculation of $3\hat{K}$ periodogram points (three-point periodogram maximization) and $\hat{K}$ sinusoid removals from the considered signal (relation (11)). On the other hand, the fine frequency estimation requires the calculation of $3\hat{K}$ periodogram points and $\hat{K}(\hat{K} - 1)$ sinusoid removals. In total, the proposed algorithm requires $\hat{K}+1$ DFTs, $\hat{K}+1$ DFT maximum detections, $6\hat{K}$ periodogram points and $\hat{K}^2$ sinusoid removals.

We assume that an $N$-samples DFT requires $N \log_2 N$ complex-valued (CV) multiplications and additions. DFT maximum detection requires $2N$ real-valued (RV) multiplications, $N$ RV additions and $N - 1$ comparisons. Calculation of one periodogram point requires $N$ CV and $N$ RV multiplications, $N$ CV exponentials and $N - 1$ CV additions. Finally, one sinusoid removal requires $N$ CV and $N$ RV multiplications, $2N - 1$ CV additions and $N$ CV exponentials. Since a CV addition requires two RV additions, a CV multiplication requires four RV multiplications and two RV additions, and a CV exponential requires two sine/cosine calculations, the overall calculation complexity of the proposed method is $[4(\hat{K} + 1)\log_2 N + 5\hat{K}^2 + 32\hat{K} + 2]N$ RV multiplications, $[4(\hat{K} + 1)\log_2 N + 6\hat{K}^2 + 25\hat{K} + 1]N$ RV additions, $2\hat{K}(\hat{K}+6)N$ sine/cosine calculations and $(\hat{K}+1)N$ comparisons.

Since $\hat{K} \ll N$, we may conclude that the algorithm complexity is $O(\hat{K}N \log_2 N)$ operations, i.e. the most expensive operation is the DFT calculation.

## IV. NUMERICAL RESULTS

In this section, the performance of model order estimation is evaluated through percentage of correct order estimation (PCOE), whereas the frequency estimation accuracy is evaluated through the mean square error (MSE) of the frequency estimation. The PCOE and MSE values are averaged over 1000 Monte-Carlo simulations. In all simulations, the threshold $T$ is set to $T = \mu_{|E|} + 6\sigma_{|E|}$, which yields the PFA of $P(|E| \geq T) = 1.459 \times 10^{-6}$. The selection of PFA, and therefore $T$, affects the method's performance. Namely, as the PFA increases, $T$ decreases, and the number of false alarms (falsely detected sinusoids) will increase. On the other side, as the PFA decreases, $T$ increases, and the number of false alarms will decrease. However, decreasing the PFA too much would lead to increased number of missed detections.

In model order estimation, the proposed method is compared to the tensor-based [25] and subspace-based [26] approaches. The setups used in [25] and [26] are adopted

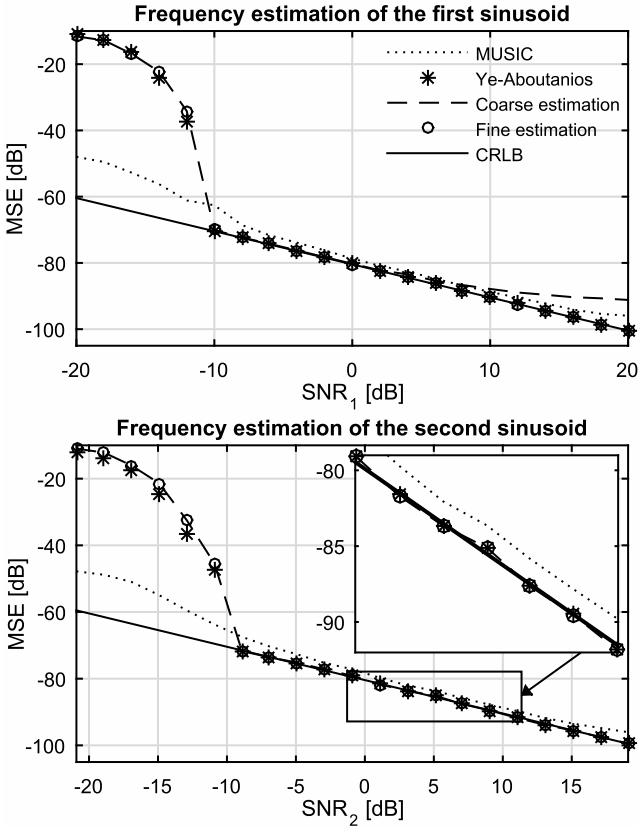


**FIGURE 1.** Frequency estimation MSE of a two-component signal versus SNR. *Top:* MSE of $f_1$. *Bottom:* MSE of $f_2$. Same legend as in the top plot.

in our simulations. In frequency estimation, the proposed method is compared to the MUSIC [13] and Ye-Aboutanios [24] estimators. The MUSIC spectrum is calculated in 32768 points using a $65 \times 65$ autocorrelation matrix constructed according to the modified covariance method [11], [30]. $Q = 2$ iterations are used in the Ye-Aboutanios method.

Let us first consider the case of two complex sinusoids with frequencies $f_1 = 0.071$ and $f_2 = 0.141$, and amplitudes $A_1 = 1$ and $A_2 = 0.9$. The signal length is $N = 256$. In each simulation, the initial phase of each complex sinusoid is chosen randomly within $(-\pi, \pi]$, which is the case for all examples in this section. Figure 1 depicts the MSE of both frequencies calculated over variable SNR. The SNR of the $k$-th sinusoid component, $\mathrm{SNR}_k$, is calculated according to

$$\mathrm{SNR}_k = \frac{A_k^2}{\sigma_\epsilon^2}. \tag{16}$$

In addition to the MSE corresponding to the overall algorithm output (fine estimation), we also present the MSE corresponding to the coarse frequency estimation. Top plot in Fig. 1 indicates that the coarse estimation itself does not suffice to achieve the CRLB. This is due to the fact that the coarse frequency estimation of stronger sinusoids is affected by the presence of weaker ones [12], [22]. This influence is

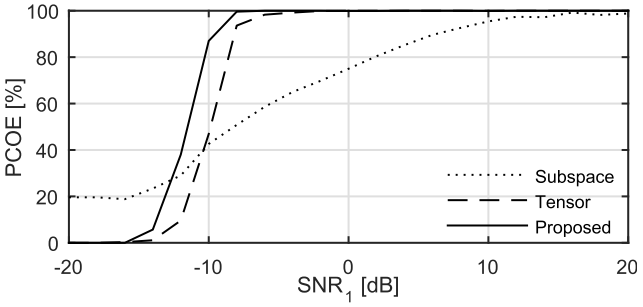


**FIGURE 2.** Percentage of correct order estimation of a two-component signal.

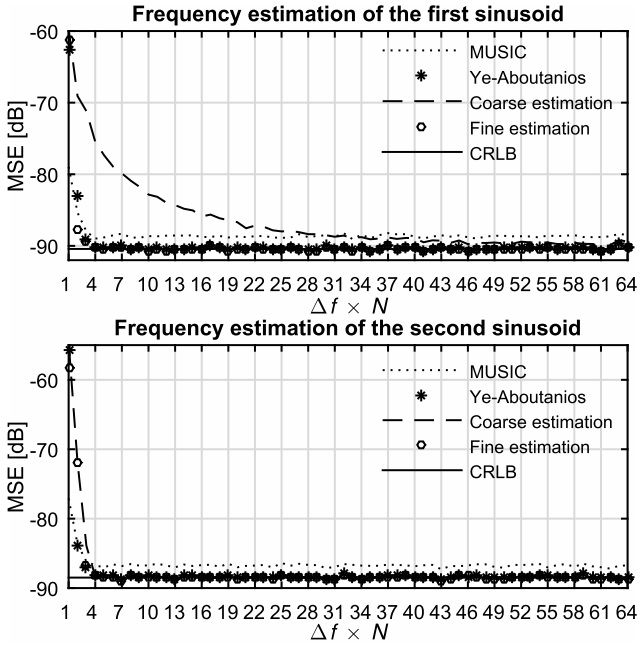


**FIGURE 3.** Frequency estimation MSE of a two-component signal versus frequency displacement $\Delta f$. *Top:* MSE of $f_1$. *Bottom:* MSE of $f_2 = f_1 + \Delta f$.

mitigated in the fine estimation stage by removing weaker sinusoids from the considered signal. The performance of the MUSIC-based estimation is very good. However, its main restriction is that the model order has to be known in advance, as in the Ye-Aboutanios method. Another disadvantage is increased numerical complexity if proper estimation accuracy is to be achieved, which depends on the autocorrelation matrix size [11]. The proposed and Ye-Aboutanios methods achieve the CRLB above the SNR threshold. Zoom window in the bottom plot of Fig. 1 shows that all considered methods, except the MUSIC-based one, perform practically the same for the weaker component. The PCOE versus SNR curves (Fig. 2) show that the proposed method outperforms both [25] and [26] in terms of order estimation accuracy.

Let us now consider a two-component signal $x(n)$ with frequencies $f_1$ and $f_2 = f_1 + \Delta f$, where $\Delta f$ represents the frequency displacement between the components. Figure 3 presents the MSE of $f_1$ (top plot) and $f_2$ (bottom plot) estimation versus $\Delta f$ varied in interval $[\frac{1}{N}, \frac{1}{4}]$ with a step $\frac{1}{N}$.

In addition, $A_1 = 1, A_2 = 0.8, N = 256$ and $\text{SNR}_1 = 10$ dB. In each run, $f_1$ is selected randomly within $(-\frac{1}{2}, \frac{1}{2})$. For both components, the proposed and Ye-Aboutanios methods achieve the CRLB, except when displacement is small. The MUSIC estimator performs very well, few dBs above the former two methods. Note also that the proposed coarse estimation of $f_1$ depends on $\Delta f$, with error hyperbolically decreasing with $\Delta f$. The MSE curves' trend for $\Delta f > \frac{1}{4}$ remains the same and is therefore not presented in Fig. 3.

**TABLE 1. Maximal MSE deviation from CRLB.**

| | $f_1$ | $f_2$ |
|---|---|---|
| MUSIC | 2.31 dB | 2.59 dB |
| Ye-Aboutanios | 0.66 dB | 0.75 dB |
| Proposed (coarse) | 7.83 dB | 0.64 dB |
| Proposed (fine) | 0.58 dB | 0.63 dB |

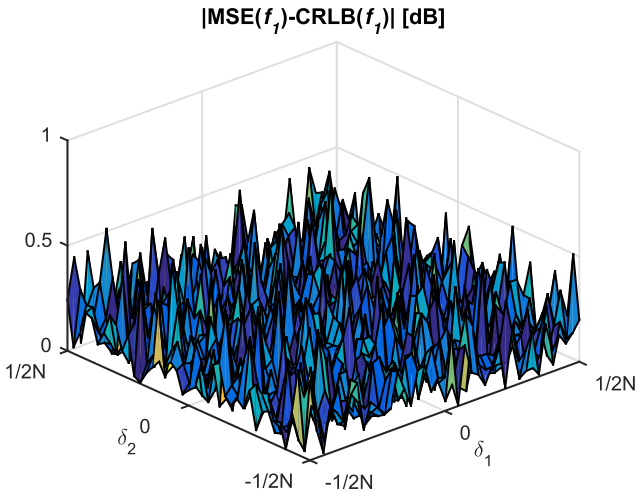


**FIGURE 4. Absolute difference between MSE and CRLB in $f_1$ estimation versus frequency offsets $\delta_1$ and $\delta_2$.**

We proceed with performance evaluation for variable offset of the sinusoid frequency from a DFT bin. In that sense, we consider a two-component signal with frequencies $f_1 = \nu_1 + \delta_1$ and $f_2 = \nu_2 + \delta_2$, where $\nu_1$ and $\nu_2$ represent frequencies corresponding to DFT bins and $\delta_1$ and $\delta_2$ offsets from $\nu_1$ and $\nu_2$, respectively. We set $\nu_1 = \frac{7}{N}$ and $\nu_2 = \frac{18}{N}$, whereas $\delta_1$ and $\delta_2$ take 41 uniformly sampled values within $[-\frac{1}{2N}, \frac{1}{2N})$. As in the previous example, $A_1 = 1, A_2 = 0.8$, $N = 256$ and $\text{SNR}_1 = 10$ dB. Table 1 reports maximal MSE deviations from the CRLB in $f_1$ and $f_2$ estimation. Absolute difference between the proposed $f_1$-estimation MSE and the corresponding CRLB (Fig. 4) is uniformly distributed over both $\delta_1$ and $\delta_2$. Its maximal value of 0.58 is very small compared to $|\text{CRLB}(f_1)|$, which is around 90 dB for this setup. Similar holds for $f_2$. The performance of the proposed method, therefore, does not depend on the frequency offset from DFT bins.

Now we consider $x(n)$ containing five sinusoids with frequencies $f_k = \{-0.088, -0.073, 0.192, 0.241, 0.378\}$ and corresponding amplitudes $A_k = \{1, 0.87, 0.61, 0.72, 0.69\}$. The signal length is $N = 1024$. One realization of the

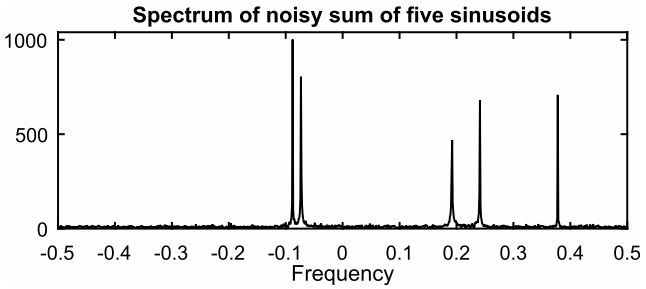


**FIGURE 5. Spectrum of a five-sinusoid signal embedded in AWGN with $\text{SNR}_1 = 10$ dB.**

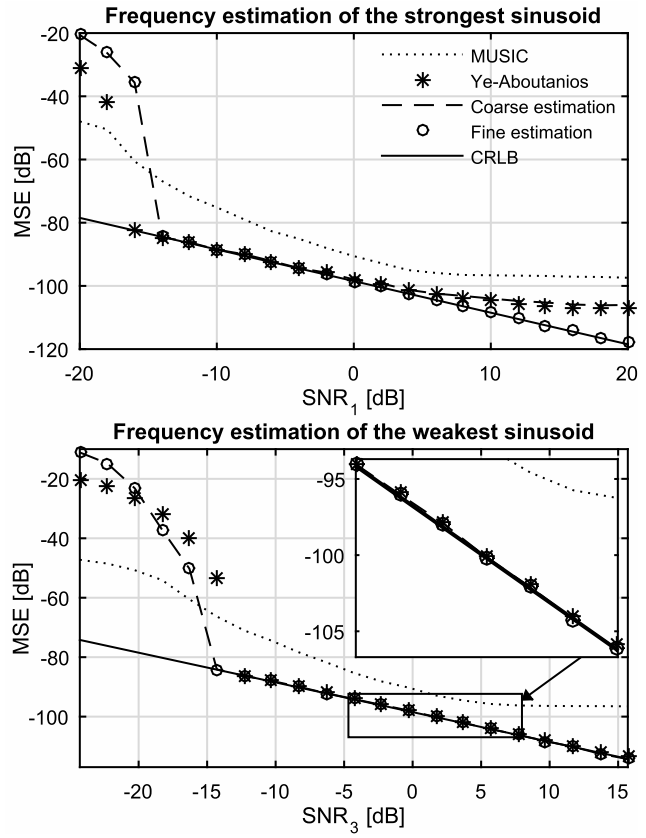


**FIGURE 6. Frequency estimation MSE of a five-component signal. *Top:* MSE of $f_1$ (strongest component). *Bottom:* MSE of $f_3$ (weakest component). Same legend as in the top plot.**

spectrum of $x(n)$, embedded in AWGN with $\text{SNR}_1 = 10$ dB, is presented in Fig. 5. Note that the strongest two components (negative frequencies) are very close to each other. Figure 6 represents the MSEs of two components versus the corresponding SNRs; top plot represents the strongest ($k = 1$) and bottom plot the weakest one ($k = 3$). For both components, as well as for three others (not presented here), the proposed method achieves the CRLB. Again, the coarse estimation itself does not suffice in achieving the CRLB, which can be seen from the top plot. Note that the Ye-Aboutanios method goes into saturation above SNR $= 2$ dB for the strongest component. This saturation appears also for other components (not presented here), except for the weakest one. For the weakest component, the proposed (both coarse and

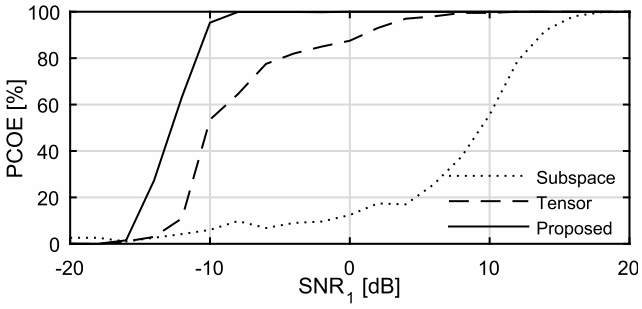


**FIGURE 7.** Percentage of correct order estimation of a five-component signal.

fine estimation) and Ye-Aboutanios methods perform practically the same (zoom window in the bottom plot of Fig. 6). Finally, the proposed method outperforms [25] and [26] in both the model order estimation accuracy and robustness to noise (Fig. 7).

From the above presented results, we can conclude that the proposed method's performance is on par with that of the Ye-Aboutanios method [24]. In addition, the calculation complexities of these two methods are of the same order $O(Order \times N \log_2 N)$, where $Order$ is the model order. As opposed to the proposed method, the Ye-Aboutanios method assumes that $Order$ is known a priori and it is characterized by MSE saturation at higher SNR (see the top plot in Fig. 6).

## V. CONCLUSIONS

A frequency-based method for detection of complex sinusoids in AWGN and their frequency estimation is proposed. Sinusoids are detected based on the Neymann-Pearson criterion. Frequency estimation of detected sinusoids, performed in the coarse and fine search stages, is based on the efficient three-point periodogram maximization approach. Apart from the DFT calculation, which represents the most expensive operation in the method, the complexity of all other operations is $O(\hat{K}^2 N)$, where the estimated model order $\hat{K}$ is usually much smaller than the signal length $N$. The proposed detection is reliable and the estimation accuracy reaches the CRLB. The future work will consider analytical derivation of the proposed frequency estimation accuracy and extension to the case of multiple 2D complex sinusoids.

## REFERENCES

[1] H. Wen, J. Zhang, Z. Meng, S. Guo, F. Li, and Y. Yang, "Harmonic estimation using symmetrical interpolation FFT based on triangular self-convolution window," *IEEE Trans. Ind. Informat.*, vol. 11, no. 1, pp. 16–26, Feb. 2015.

[2] P. Stoica, R. L. Moses, B. Friedlander, and T. Soderstrom, "Maximum likelihood estimation of the parameters of multiple sinusoids from noisy measurements," *IEEE Trans. Acoust., Speech Signal Process.*, vol. 37, no. 3, pp. 378–392, Mar. 1989.

[3] S. Djukanović, M. Simeunović, and I. Djurović, "Refinement in the estimation of multicomponent polynomial-phase signals," in *Proc. IEEE Int. Conf. Acoust., Speech Signal Process. (ICASSP)*, Mar. 2012, pp. 3957–3960.

[4] Z. Marzi, D. Ramasamy, and U. Madhow, "Compressive channel estimation and tracking for large arrays in mm-wave picocells," *IEEE J. Sel. Topics Signal Process.*, vol. 10, no. 3, pp. 514–527, Apr. 2016.

[5] S. Montagner, N. Benvenuto, and S. Tomasin, "Taming the complexity of mm-wave massive MIMO systems: Efficient channel estimation and beamforming," in *Proc. IEEE Int. Conf. Commun. Workshop (ICCW)*, Jun. 2015, pp. 1251–1256.

[6] A. Pelinković, S. Djukanović, I. Djurović, and M. Simeunović, "A frequency domain method for the carrier frequency offset estimation in OFDM systems," in *Proc. 8th Int. Symp. Image Signal Process. Anal. (ISPA)*, Sep. 2013, pp. 326–330.

[7] U. Mengali and M. Morelli, "Data-aided frequency estimation for burst digital transmission," *IEEE Trans. Commun.*, vol. 45, no. 1, pp. 23–25, Jan. 1997.

[8] C. Hackman, J. Levine, T. E. Parker, D. Piester, and J. Becker, "A straightforward frequency-estimation technique for GPS carrier-phase time transfer," *IEEE Trans. Ultrason., Ferroelectr., Freq. Control*, vol. 53, no. 9, pp. 1570–1583, Sep. 2006.

[9] N. Ostlund, J. Yu, and J. S. Karlsson, "Improved maximum frequency estimation with application to instantaneous mean frequency estimation of surface electromyography," *IEEE Trans. Biomed. Eng.*, vol. 51, no. 9, pp. 1541–1546, Sep. 2004.

[10] K. Duda, L. B. Magalas, M. Majewski, and T. P. Zielinski, "DFT-based estimation of damped oscillation parameters in low-frequency mechanical spectroscopy," *IEEE Trans. Instrum. Meas.*, vol. 60, no. 11, pp. 3608–3618, Nov. 2011.

[11] P. Stoica and R. Moses, *Spectral Analysis of Signals*. Upper Saddle River, NJ, USA: Prentice-Hall, 2005.

[12] D. C. Rife and R. R. Boorstyn, "Multiple tone parameter estimation from discrete-time observations," *Bell Syst. Tech. J.*, vol. 55, no. 9, pp. 1389–1410, Nov. 1976.

[13] R. O. Schmidt, "Multiple emitter location and signal parameter estimation," *IEEE Trans. Antennas Propag.*, vol. AP-34, no. 3, pp. 276–280, Mar. 1986.

[14] R. Roy and T. Kailath, "Esprit-estimation of signal parameters via rotational invariance techniques," *IEEE Trans. Acoust., Speech, Signal Process.*, vol. 37, no. 7, pp. 984–995, Jul. 1989.

[15] S. Huang, H. Zhang, H. Sun, L. Yu, and L. Chen, "Frequency estimation of multiple sinusoids with three sub-Nyquist channels," *Signal Process.*, vol. 139, pp. 96–101, Oct. 2017.

[16] J. Selva, "ML estimation and detection of multiple frequencies through periodogram estimate refinement," *IEEE Signal Process. Lett.*, vol. 24, no. 3, pp. 249–253, Mar. 2017.

[17] D. C. Rife and R. R. Boorstyn, "Single tone parameter estimation from discrete-time observations," *IEEE Trans. Inf. Theory*, vol. IT-20, no. 5, pp. 591–598, Sep. 1974.

[18] B. G. Quinn, "Estimation of frequency, amplitude, and phase from the DFT of a time series," *IEEE Trans. Signal Process.*, vol. 45, no. 3, pp. 814–817, Mar. 1997.

[19] E. Aboutanios and B. Mulgrew, "Iterative frequency estimation by interpolation on Fourier coefficients," *IEEE Trans. Signal Process.*, vol. 53, no. 4, pp. 1237–1242, Apr. 2005.

[20] C. Candan, "Analysis and further improvement of fine resolution frequency estimation method from three DFT samples," *IEEE Signal Process. Lett.*, vol. 20, no. 9, pp. 913–916, Sep. 2013.

[21] Ç. Candan, "Fine resolution frequency estimation from three DFT samples: Case of windowed data," *Signal Process.*, vol. 114, pp. 245–250, Sep. 2015.

[22] S. Djukanović, "An accurate method for frequency estimation of a real sinusoid," *IEEE Signal Process. Lett.*, vol. 23, no. 7, pp. 915–918, Jul. 2016.

[23] S. Djukanović, "Sinusoid frequency estimator with parabolic interpolation of periodogram peak," in *Proc. 40th Int. Conf. Telecommun. Signal Process. (TSP)*, Jul. 2017, pp. 470–473.

[24] S. Ye and E. Aboutanios, "Rapid accurate frequency estimation of multiple resolved exponentials in noise," *Signal Process.*, vol. 132, pp. 29–39, Mar. 2017.

[25] E. A. Ince, M. K. Allahdad, and R. Yu, "A tensor approach to model order selection of multiple sinusoids," *IEEE Signal Process. Lett.*, vol. 25, no. 7, pp. 1104–1108, Jul. 2018.

[26] M. G. Christensen, A. Jakobsson, and S. H. Jensen, "Sinusoidal order estimation using angles between subspaces," *EURASIP J. Adv. Signal Process.*, vol. 2009, Nov. 2009, Art. no. 948756.

[27] A. Papoulis and U. S. Pillai, *Probability, Random Variables, and Stochastic Processes*, 4th ed. New York, NY, USA: McGraw-Hill, 2002.
[28] S. Djukanović and V. Popović, "A parametric method for multicomponent interference suppression in noise radars," *IEEE Trans. Aerosp. Electron. Syst.*, vol. 48, no. 3, pp. 2730–2738, Jul. 2012.
[29] S. Djukanović, T. Popović, and A. Mitrović, "Precise sinusoid frequency estimation based on parabolic interpolation," in *Proc. 24th Telecommun. Forum (TELFOR)*, Nov. 2016, pp. 1–4.
[30] S. L. Marple, *Digital Spectral Analysis: With Applications*, vol. 5. Englewood Cliffs, NJ, USA: Prentice-Hall, 1987.

**SLOBODAN DJUKANOVIĆ** was born in Valjevo, Serbia, in 1976. He received the B.Sc., M.Sc., and Ph.D. degrees in electrical engineering from the University of Montenegro, Podgorica, in 2001, 2004, and 2008, respectively.

He is currently an Associate Professor with the Faculty of Electrical Engineering, University of Montenegro. From 2008 to 2009, he was in Grenoble, France, where he finished his Postdoctoral studies at the GIPSA-Lab, CNRS. His research concerns parameter estimation, time-frequency signal analysis, and machine learning.

**VESNA POPOVIĆ-BUGARIN** was born in Podgorica, Montenegro, in 1978. She received the B.Sc., M.Sc., and Ph.D. degrees in electrical engineering from the University of Montenegro in 2001, 2005, and 2009, respectively.

She is currently an Associate Professor with the Faculty of Electrical Engineering, University of Montenegro. Her research interests include time–frequency signal analysis, SAR/ISAR imaging, micro-Doppler analysis, parameter estimation, data mining, and expert systems.